ADVANCED FUNCTIONAL MATERIALS

DOI: 10.1002/adfm.200500478

Fibrillar Growth in Polyaniline**

By *Xinyu Zhang*, *Harsha S. Kolla*, *Xianghui Wang*, *Kirtana Raja*, and *Sanjeev K. Manohar**

Large, colorless aggregates are observed during the induction period of a chemical oxidative polymerization of aniline in dilute aqueous acids using an ammonium peroxydisulfate oxidant. Observed for the first time by static and dynamic light-scattering (LS) measurements, these aggregates are believed to be anilinium–peroxydisulfate ion clusters whose shape (spherical or rod-like) plays an important role in the overall morphology of the emeraldine salt formed (granular or fibrillar). The role of these aggregates in influencing the morphology of polyaniline is further evaluated under a variety of reaction conditions, for example, varying ionic strength, concentration, temperature, nitrogen substitution, and so forth.

1. Introduction

Chemical oxidative polymerization of aniline in dilute aqueous acids using an ammonium peroxydisulfate oxidant proceeds via the intermediacy of large, colorless aggregates that act as 'seeds' in orchestrating the overall morphology of the product polyaniline. Observed for the first time by continuously monitoring the polymerization by static and dynamic light-scattering (LS) measurements, these aggregates are formed during the induction period just prior to the onset of polymerization and are believed to be aggregates of the anilinium cation and the peroxydisulfate anion. Depending on the reaction conditions, these aggregates can be spherical or rod-like with the latter leading to polyaniline with a bulk nanofibrillar morphology. These findings expand the role of our recently described 'nanofiber-seeding' method in which small quantities (seeds) of insoluble materials with nanofibrillar morphology seeds added just prior to the onset of polymerization help orchestrate bulk fibrillar polymer growth.[1] Even conventional polyaniline nanofiber synthesis could be viewed as a 'seeded-polymerization' system, only this time the seeds are aggregates formed in situ during the early stages of the reaction. The intermediacy of these aggregates provides an important synthetic vector that can be leveraged to control nanoscale morphology in these systems.[2]

There are several synthetic approaches to the chemical synthesis of polyaniline nanofibers, for example, interfacial polymerization,[3,4] nanofiber seeding,[1] oligomer-assisted polymerization,[5] surfactant-assisted polymerization,[6] and nontemplate polymerization.[7] The polyaniline system is particularly prone to fibrillar polymer growth[1,4,8] compared to other conducting-polymer systems such as polypyrrole, poly(3,4-ethylenedioxythiophene), and polythiophene; for example, it has recently been reported that nanofibers are obtained by carrying out the reaction under dilute reaction conditions[9] in the absence of templates. In one report it was shown that under relatively dilute conditions, while nanofibers are obtained when the oxidant peroxydisulfate is added all at once, only granular polyaniline is obtained when it is added dropwise.[10] The rationale offered was that when the oxidant is added dropwise, secondary polymerization processes begin to disrupt the primary process, namely, fibrillar polymer growth that is favored when the oxidant is added all at once. However, in these reports, including those from our group, there has not been a clear mechanistic rationale for nanofiber formation in the polyaniline system, and, particularly, reasons why fibrillar polymer growth is intrinsically favored in the polyaniline system over other conducting-polymer systems are lacking. It is also important to note that in spite of the diversity in the synthetic approaches outlined above, the polyaniline nanofibers have strikingly similar morphology, that is, they generally precipitate from the reaction mixture as a mat composed of 30–60 nm diameter nanofibers. We believe this points to a common underlying mechanism.

In our earlier reports on the synthesis of polyaniline nanofibers, we raised the possible role of the soluble aniline dimer intermediate, *N*-phenylphenylenediamine,[1,4] in directing fibrillar polymer growth. This was based on an early study on electrochemically synthesized polyaniline where addition of small amounts of aniline dimer resulted in fibrillar polyaniline.[11] While the role of the aniline dimer was unclear at that time, we believe that the process by which the dimer is formed, that is, processes governing the induction period of the reaction, could be important in the evolution of the bulk polymer morphology.

[*] Prof. S. K. Manohar, Dr. X. Zhang, H. S. Kolla, X. Wang, K. Raja
Department of Chemistry, Alan G. MacDiarmid Center for Innovation
The University of Texas at Dallas
Richardson, TX 75080 (USA)
E-mail: sanjeev.manohar@utdallas.edu

[**] We thank Prof. A. G. MacDiarmid, Dr. G. R. Dieckmann and Dr. M. Chen of Wyatt Technology Corp. for helpful discussions and The University of Texas at Dallas for financial support.

2. Results and Discussion

2.1. Reaction Profiling Using LS

We used static and dynamic LS simultaneously to monitor two aniline polymerization systems, one yielding fibrillar polyaniline, and the other yielding granular polyaniline. This was done in an effort to determine if any molecular aggregates were formed during the very early stages of the reaction, and if meaningful conclusions could be drawn from differences between these two systems. There are significant challenges to this approach, for not only should all reagents and solvents be free of particulate matter, but the polymerization kinetics should be sufficiently slow to obtain meaningful results. There should also be a clear difference in polymer morphology in these two systems. In addition, any colored intermediate species would interfere with the 690 nm laser light source, and there is a limited time window prior to the onset of polymerization in which reliable LS data can be obtained. For example, Figure 1, curve 1 shows the potential–time profile of a chemical oxidative polymerization of aniline carried out under dilute conditions. The reaction proceeds by: i) a colorless induction period of ca. 30 min in which LS data can be used, ii) the appearance of a pale-green or blue-green color, presumably an aniline radical cation or aniline dimer, over a period of 2–3 min, beyond which LS measurements cannot be used, and iii) an abrupt darkening of the reaction mixture accompanied by a rapid bulk precipitation of polyaniline.[12] It was important to identify synthetic conditions under which the colorless induction period was sufficiently long to enable reliable LS measurements to be made. Oxidative polymerization in aqueous 1 M HCl was studied by changing the following five synthetic parameters: i) adding aniline dimer prior to the onset of polymerization, ii) temperature, iii) concentration, iv) ionic strength,[13] and v) using a *N*-methylaniline derivative. The system best suited for LS was a room-temperature polymerization of aniline carried out at low reagent concentrations (0.022 M aniline) in the presence and absence of added 3 M NaCl.

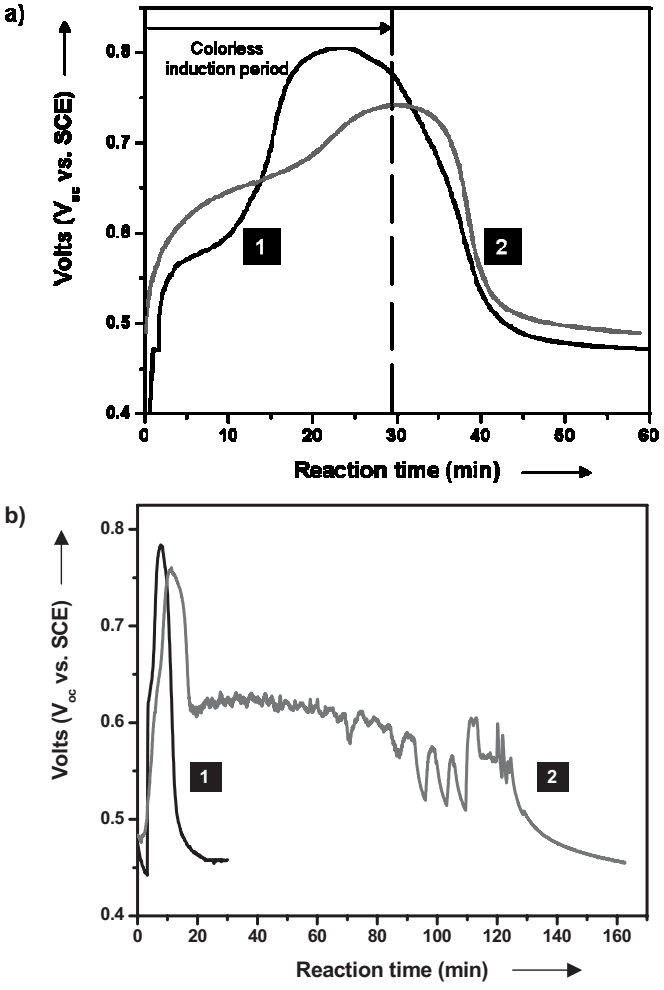

Figure 1. Potential–time profile of aniline polymerization in aqueous 1 M HCl: a) control, salt-free conditions (1) and with added 3 M NaCl (2), aniline (0.022 M), $(NH_4)_2S_2O_8$ (0.005 M), and b) oxidant added all at once (1) and dropwise (2), aniline (0.22 M), $(NH_4)_2S_2O_8$ (0.05 M). V_{oc}: open-circuit potential; SCE: saturated calomel electrode.

2.2. Effect of Ionic Strength on Polyaniline Morphology

The salt-free system yielded polyaniline with a nanofibrillar morphology while addition of 3 M NaCl resulted in a predominantly granular morphology (Fig. 2). Continuous monitoring of the reaction of the salt-free system by static and dynamic LS is shown in Figure 3a and the analogous plots for the 3 M NaCl system are shown in Figure 3b. Duplicates of these reactions were also carried out simultaneously with the potential–time profiles being monitored continuously [12] (Fig. 1a). This was done in order to obtain both a visual read of the polymerization, and information on the intermediacy of any oxidized aniline species during the polymerization (Fig. 3, vials). The simultaneous visual read confirmed that the time period corresponding to the rise in intensity of the scattered light in

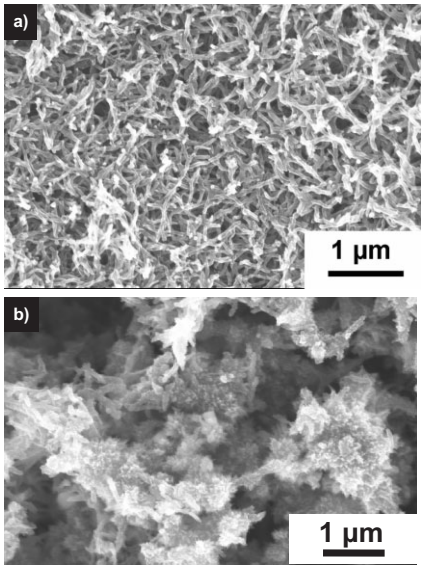

Figure 2. SEM images of polyaniline (emeraldine·HCl) powder synthesized: a) under salt-free conditions (control) and b) with added 3 M NaCl.

ADVANCED FUNCTIONAL MATERIALS

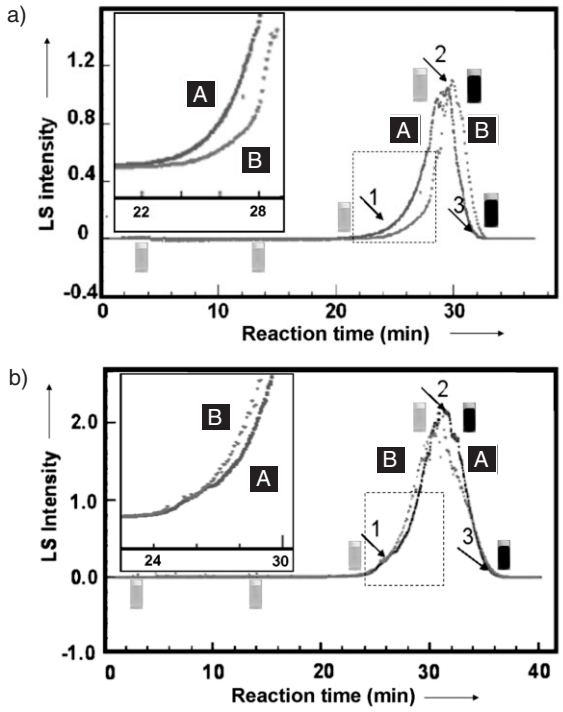

Figure 3. Continuous monitoring of aniline polymerization with time by static (A) and dynamic (B) LS in aqueous 1 M HCl: a) salt-free conditions, b) with added 3 M NaCl. Insets: expanded regions of interest.

Figure 3, from points 1 to 2, corresponds to the colorless induction period, while the subsequent fall in light intensity, from points 2 to 3, corresponds to when the blue-colored intermediate is formed and begins to interfere with the measurements. Reliable LS data can only be obtained from the start of the reaction until the time corresponding to point 2. Simultaneous potential–time profiling confirmed that the LS measurements were made while the open-circuit potential (V_{oc}) was still high (and rising), and well before the formation of the highly colored aniline dimer or polyaniline in the pernigraniline oxidation state. Both systems show the intermediacy of very large aggregates, ranging in size from 25 to 70 nm (Table 1). There is also a reversal in the magnitude of static LS values for radius of gyration (R_g) values and dynamic LS values for hydrodynamic radii (R_h) between the salt-free and 3 M NaCl systems. The ratio R_g/R_h, which in classical LS is a measure of the shape of the aggregate/solute,[14,15] shows that the salt-free system proceeds through the intermediacy of non-spherical, rodlike aggregates ($R_g/R_h = 2.5$), while the 3 M NaCl system proceeds via the intermediacy of spherical aggregates ($R_g/R_h = 0.8$). Spherical aggregates would favor isotropic polymer growth (granular morphology) over anisotropic growth (fibrillar morphology), and we believe that the high ionic strength in the 3 M NaCl system would screen out any anisotropic solution effects during the early stages of the reaction. This rationale is also consistent with a recent report on polyaniline nanofibers (salt-free system) in which anisotropic growth is believed to result from a "depleted-solution" region along the length of a growing fiber chain, and in which fresh polymer growth takes place preferably at the ends of the fiber.[16] The soluble aggregates are not present at the beginning of the reaction, but are formed just prior to the formation of the blue-colored intermediate species. Their size increases with reaction time (Table 1), consistent with a clustering phenomenon of some type.

Table 1. Radius of gyration (R_g) and hydrodynamic radius (R_h) of aggregates formed during the induction period of the chemical oxidative polymerization of aniline.

System	Time [min]	R_g [nm]	R_h [nm]	R_g/R_h
Salt-free	24.0	76.8	25.4	3.0
	30.0	93.5	37.3	2.5
3 M NaCl	26.0	60.5	46.2	1.3
	32.0	61.5	69.6	0.88

2.3. Aggregate Formation in Solution

In aqueous 1 M acid, aniline monomer is present in solution predominantly as the anilinium ion, $(C_6H_5NH_3)^+$. We postulate that when $(NH_4)_2S_2O_8$ is first added to an aqueous acidic solution of aniline, a series of equilibrium ion-exchange reactions takes place between H^+, NH_4^+, $(C_6H_5NH_3)^+$, and $S_2O_8^{2-}$ ions. Both monodianilinium peroxydisulfate, $(NH_4)(C_6H_5NH_3)S_2O_8$, and dianilinium peroxydisulfate, $(C_6H_5NH_3)_2S_2O_8$, can be formed. In the presence of added 3 M NaCl, $Na(C_6H_5NH_3)S_2O_8$ can also be formed, and the relative proportions of the various species in solution is a function of ionic strength. In salt-free systems, we believe the equilibrium favors $(C_6H_5NH_3)_2S_2O_8$ formation (Eq. 2), while in 3 M NaCl the equilibrium favors $Na(C_6H_5NH_3)S_2O_8$ formation (Eq. 4).

Under salt-free conditions:

$$(NH_4)_2S_2O_8 + C_6H_5NH_3^+Cl^- \rightleftharpoons (NH_4)(C_6H_5NH_3)S_2O_8 + NH_4Cl \quad (1)$$

$$(NH_4)(C_6H_5NH_3)S_2O_8 + C_6H_5NH_3^+Cl^- \rightleftharpoons (C_6H_5NH_3)_2S_2O_8 + NH_4Cl \quad (2)$$

In 3 M NaCl:

$$(NH_4)_2S_2O_8 + 2\,NaCl \rightleftharpoons Na_2S_2O_8 + 2\,NH_4Cl \quad (3)$$

$$Na_2S_2O_8 + C_6H_5NH_3^+Cl^- \rightleftharpoons Na(C_6H_5NH_3)S_2O_8 + NaCl \quad (4)$$

Complex formation between cationic ammonium ions and anionic $S_2O_8^{2-}$ ions has been observed previously; for example, cationic surfactants such as RMe_3N^+ have been shown to ion exchange with $S_2O_8^{2-}$ ions, yielding precipitates of $(RMe_3N)_2S_2O_8$ that can be isolated.[17] We have also recently isolated $RMe_3N^+Br^-$ salts with varying straight-chain R groups. Chain lengths above C_{12} yield isolable white precipi-

tates while chain lengths of C_{10} and C_8 are soluble. In addition, when $R = C_{10}H_{22}$ or C_8H_{20}, the $[(R)Me_3N]_2S_2O_8$ formed further aggregates in solution to yield large clusters, some with $R_g \sim 25$ nm.

Based on this mechanistic rationale, we believe aggregates formed from $(C_6H_5NH_3)_2S_2O_8$ yield polyaniline with a fibrillar morphology (salt-free system), while those formed from $Na(C_6H_5NH_3)S_2O_8$ yield polyaniline with a granular morphology (3 M NaCl system). The small amount of nanofibers observed even in the 3 M NaCl system can be attributed to aggregates from both mono- and dianilinium peroxydisulfate species present in equilibrium. LS measurements show that $Na(C_6H_5NH_3)S_2O_8$ aggregates are largely spherical ($R_g/R_h = 0.8$); $Na(C_6H_5NH_3)S_2O_8$ can be viewed as a conventional single-tailed surfactant with a hydrophilic $NaS_2O_8^-$ head and hydrophobic anilinium tail. In contrast, aggregates from $(C_6H_5NH_3)_2S_2O_8$ are rodlike ($R_g/R_h = 2.5$), since its dumbbell shape resembles twin-tailed (gemini) surfactants. Gemini surfactants have been shown to form nonspherical, ellipsoidal aggregates in solution.[18] In addition, $(C_6H_5NH_3)_2S_2O_8$ should be able to form large 2D aggregates in solution (Fig. 4), in which both benzene rings can participate in π–π stacking. While both aggregate types should be able to increase the dimensionality by clustering along the z-direction and increasing in size (as is experimentally observed), our working hypothesis is that fibrillar polymer growth is favored when aggregates formed from $(C_6H_5NH_3)_2S_2O_8$ are sufficiently soluble in the reaction mixture. These soluble (or highly dispersible) species act as seeds that promote fibrillar polymer growth. It is to be noted that the analogy to conventional surfactants is qualitative at best, in view of the much larger aggregate size (25–70 nm) observed in the polymerization system compared to conventional surfactants (2–10 nm).

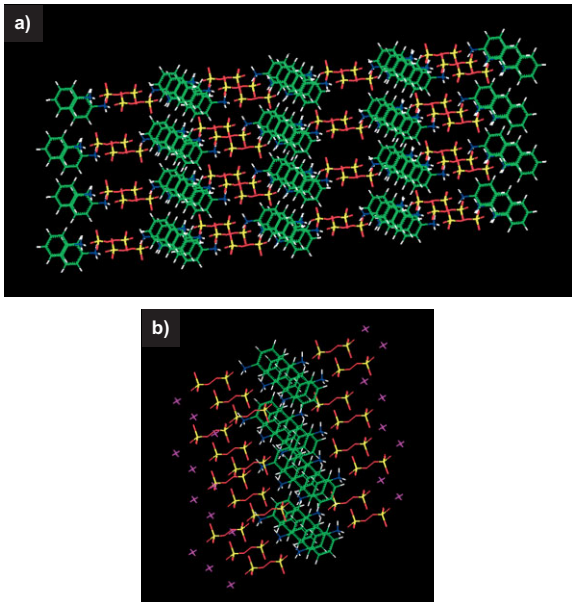

Figure 4. 3D models describing aggregation phenomena in: a) bisanilinium peroxydisulfate and b) monoanilinium peroxydisulfate. Color code: green (C): blue (N), red (O), yellow (S), purple (Na^+).

It is still unclear precisely how these aggregates form spontaneously and seed further polymer growth, although experimental evidence is consistent with the configuration outlined in Figure 4 and Scheme 1. The amine groups of adjacent rings are poised for 1,4-ring coupling and rapid chain growth immediately following the induction period (as is observed). In addition, ring coupling is expected to take place along the π-stacked benzene rings, which translates to extending the length of the fiber (edges of the scroll) as opposed to its width. We also observe an empirical correlation between fiber diameter and R_h values of $(C_6H_5NH_3)_2S_2O_8$ aggregates, whose genesis is unclear at the present time. For example, polyaniline nanofibers with an average fiber diameter in the 50–70 nm range is observed in systems in which aggregates with R_h values in the 25–37 nm range are also observed. It is possible that aggregates of $(C_6H_5NH_3)_2S_2O_8$ are sufficiently hydrophobic for R_h values to be free from the effects of a large solvation shell. These values would therefore reflect the actual aggregate size in solution, permitting one to make a connection between R_h values and average fiber diameter.

2.4. Soluble Aggregates versus Seeding Polymerization

The role of soluble rodlike aggregates in orchestrating fibrillar polymer growth in salt-free systems could be viewed as a variant of our recently reported 'nanofiber-seeding' method,[1] in which small (seed) amounts of insoluble solid nanofibers of known chemical composition are deliberately added to the reaction mixture to initiate fibrillar polymer growth. The mechanistic trajectory is peculiar to these precipitation polymerization systems in which the loci of a growing chain shifts from solution to an already existing chain, that is, the oxidation potential of the oligomer is lower than that of the monomer. So, once mono- or dianilinium peroxydisulfate aggregates initiate aniline oxidation and the first aniline oligomer precipitate is formed, subsequent polymerization will take place along the edges of this precipitate whose morphology, as we have seen, is determined by the general shape of the seed aggregates. The model in Figure 4 also helps explain the near-quantitative para coupling observed under acidic conditions, that is, not only are the positively charged anilinium groups pointing away from one another but aromatic π-stacking locks them in a specific configuration (Scheme 1).

The relative differences in the magnitude of the R_g and R_h values obtained provide additional evidence for the intermediacy of aggregates based on $Na(C_6H_5NH_3)S_2O_8$ versus $(C_6H_5NH_3)_2S_2O_8$. In classical LS, while R_g reflects the mass distribution of the aggregate in solution, R_h includes contribution from the solvation shell as well.[15] Aggregates of $Na(C_6H_5NH_3)S_2O_8$ are expected to be smaller in size (smaller R_g) but in view of the charged 'headgroup', would have a larger solvation shell (larger R_h) compared to $(C_6H_5NH_3)_2S_2O_8$. Experimental evidence consistent with this rationale is described in Table 1, where aggregates in the 3 M NaCl system have a smaller R_g value ($R_g = 60.5$ nm) compared to the salt-free system ($R_g = 76.8$ nm). In contrast, aggregates in the 3 M NaCl sys-

ADVANCED FUNCTIONAL MATERIALS

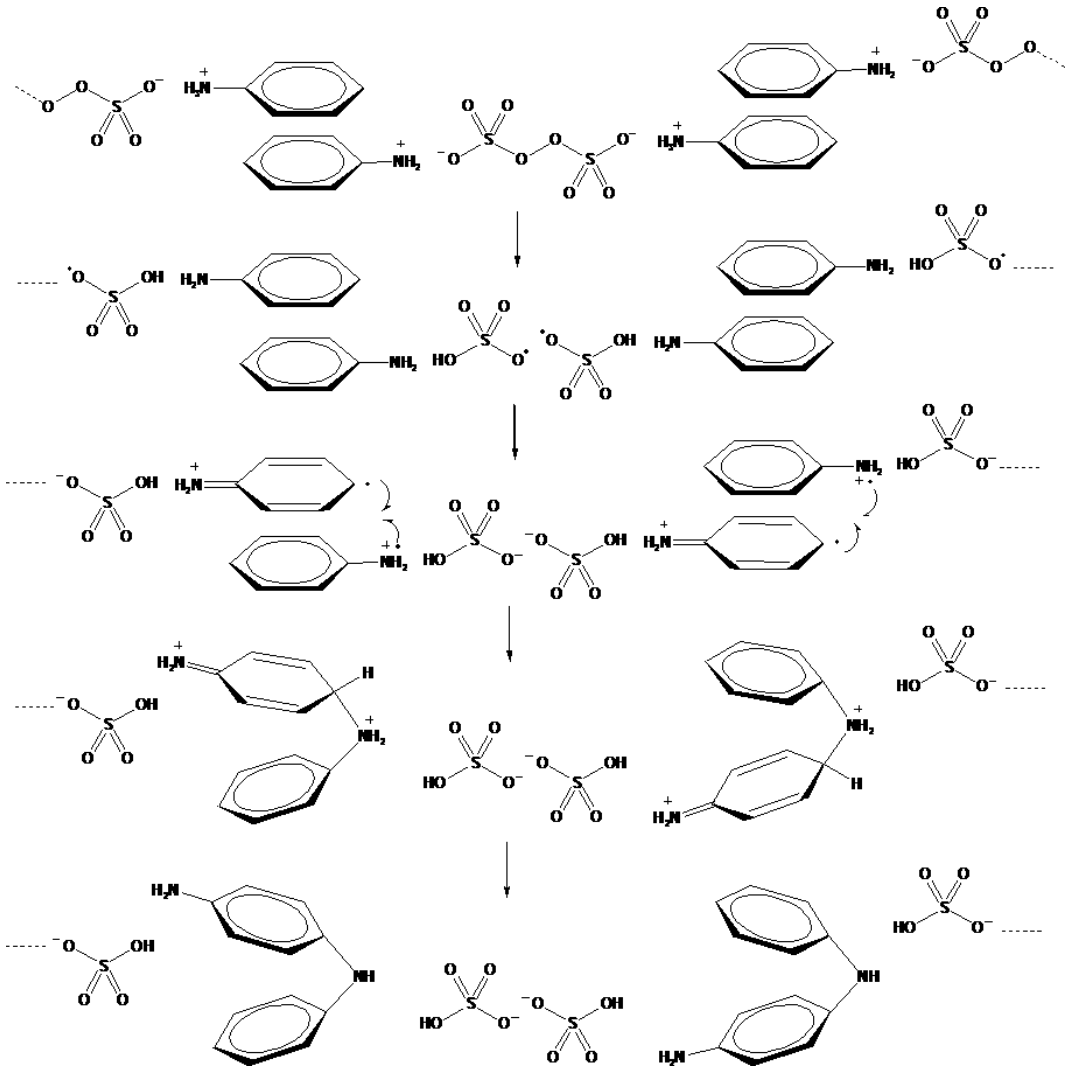

Scheme 1. Proposed mechanism of aniline polymerization proceeding via the intermediacy of dianilinium peroxydisulfate.

tem have a larger R_h value ($R_h = 46.2$ nm) compared to the salt-free system ($R_h = 25.4$ nm). It is to be noted that this mechanism calls for the initial coupling of two aniline units to take place between two adjacent aniline/S_2O_8 aggregates and once this coupling yields the aniline dimer intermediate, fresh $S_2O_8^{2-}$ ions would rapidly reform the aggregate in view of the lower oxidation potential of the dimer, that is, aniline oligomers and growing chains would constantly be surrounded by peroxydisulfate ions until the completion of the reaction. These dimer- or oligomer-based aggregates would also be strongly aggregated until the completion of the reaction and one expects the original seed morphology of the oligomer to be transcribed to the bulk precipitate. When aniline dimer is added to a solution of aniline and aqueous 1 M HCl prior to addition of peroxydisulfate, rodlike aggregates are formed in solution and one obtains polyaniline with bulk nanofibrillar morphology.[19]

2.5. Temperature and Concentration Effects on Polyaniline Morphology

At a given concentration, higher reaction temperatures (in salt-free environments) favor nanofiber formation and scanning electron microscopy (SEM) images for the parent polyaniline systems are shown in Figure 5. This is consistent with i) a greater relative concentration of $(C_6H_5NH_3)_2S_2O_8$ (Eq. 2 driven to completion) and ii) an increased solubility and ordering of $(C_6H_5NH_3)_2S_2O_8$ aggregates. The effect is even more dramatic in the poly(*N*-methylaniline) system (Fig. 5), where there is a change from spherical to fibrillar morphology as the temperature is increased.

At a given temperature, the effect of concentration on morphology for the parent polyaniline and poly(*N*-methylaniline) systems is shown in Figure 6 (also in a salt-free environment). One observes a transition from granular to fibrillar morphol-

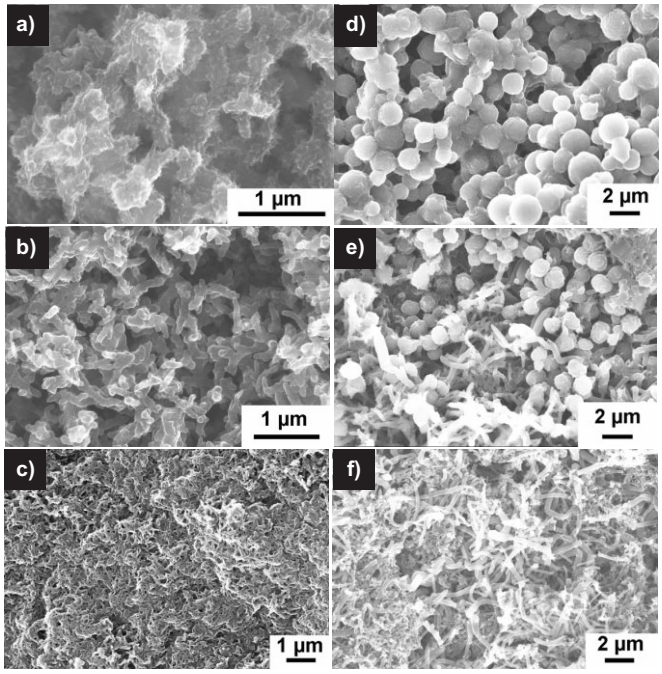

Figure 5. SEM images of parent polyaniline (a,b,c) and poly(*N*-methylaniline) (d,e,f) powder synthesized under salt-free conditions at different reaction temperatures: a,d) 0 °C; b,e) 22 °C; and c,f) 55 °C.

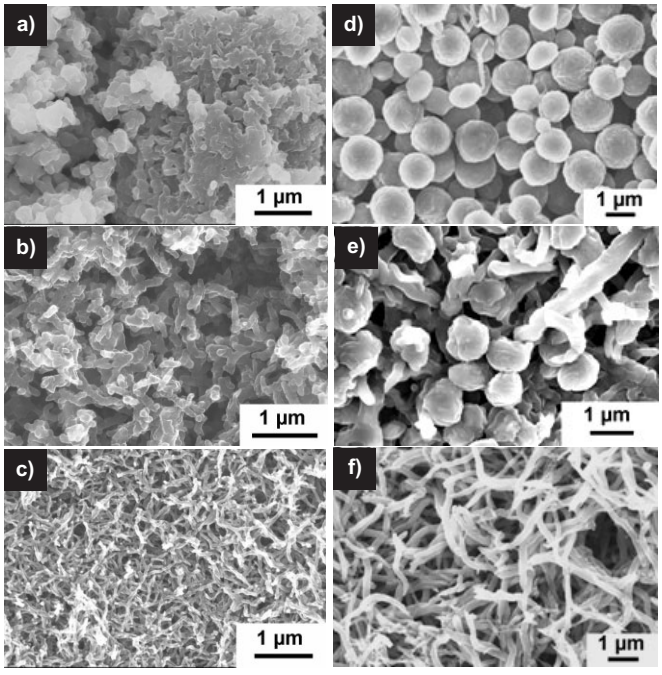

Figure 6. SEM images of parent polyaniline (a,b,c) and poly(*N*-methylaniline) (d,e,f) powder synthesized under salt-free conditions at different monomer concentrations: a) 0.43, b) 0.22, c) 0.022, d) 0.36, e) 0.18, f) 0.09 M.

ogy upon simply diluting the reaction mixture from 0.43 to 0.022 M, which is qualitatively similar with previously published results.[9,20] The effect, once again, is quite dramatic in the poly(*N*-methylaniline) system where the transition is from spherical to fibrillar morphology. The effects of dilution on polyaniline morphology can be rationalized on temporal grounds where the long induction period permits the gradual formation and aggregation of $(C_6H_5NH_3)_2S_2O_8$ prior to the onset of polymerization. While at first glance fibrillar polymer growth under dilute conditions appears to be related to a reduction in the kinetics of polymerization compared to in more concentrated conditions, potential profiling of these systems shows that this is not the case (Fig. 1a). Compared to the 3 M NaCl system (granular morphology), polymerization occurs much more rapidly under salt-free conditions (fibrillar morphology). Similarly, other fiber-yielding systems, for example, high-temperature, dimer-seeded, and so on forth, also display faster reaction kinetics.[19]

2.6. Role of Gradual Addition of Oxidant on Polyaniline Morphology

These findings are consistent with a recently published report on granular polyaniline obtained when $(NH_4)_2S_2O_8$ was added gradually (as opposed to all at once).[20] Nanofibers were formed initially, but subsequent addition of $(NH_4)_2S_2O_8$ yielded granular polyaniline which was reported to be caused by secondary chain-growth processes. We too observe qualitatively similar results under our modified conditions. However, we attribute the secondary growth process to contributions from the intermediate pernigraniline that is formed, and not to the primary reaction between aniline and $(NH_4)_2S_2O_8$. When $(NH_4)_2S_2O_8$ is added gradually, the initial oxidation of aniline would yield a small amount of fibrillar polyaniline consistent with our proposed mechanism involving $(C_6H_5NH_3)_2S_2O_8$ aggregates (the primary reaction). These 'early' nanofibers are expected to be in the emeraldine oxidation state, as is consistent with the green color observed in these nanofibers. Since the oxidation potential of emeraldine nanofibers is lower than the aniline monomer, any added peroxydisulfate would immediately be consumed in the conversion of these nanofibers to the pernigraniline oxidation state. As we have shown before, the oxidation potential of pernigraniline is sufficiently high to oxidize fresh aniline monomer to polyaniline.[12] The pernigraniline nanofibers would be reduced back to emeraldine (Scheme 2). We believe this would constitute a secondary growth process, one in which pernigraniline would be an in situ oxidant that is generated upon addition of fresh $(NH_4)_2S_2O_8$. Since no excess $(NH_4)_2S_2O_8$ was present in the reaction mixture to form aggregates with the aniline monomer, no nanofibers were obtained.

Potential-profiling results are consistent with this rationale (Fig. 1). When $(NH_4)_2S_2O_8$ is added all at once, the potential of the system reaches 0.77 V (vs. the saturated calomel electrode (SCE)) over a period of 8 min (pernigraniline oxidation state), and then falls to 0.46 V (emeraldine oxidation state). We previously showed that 80 % of the bulk polymerization occurs when the potential is high (0.77 V) when aniline is converted to pernigraniline.[12] Since there is an excess of aniline monomer in the reaction (aniline/$(NH_4)_2S_2O_8$ ratio ~4:1), all

ADVANCED FUNCTIONAL MATERIALS

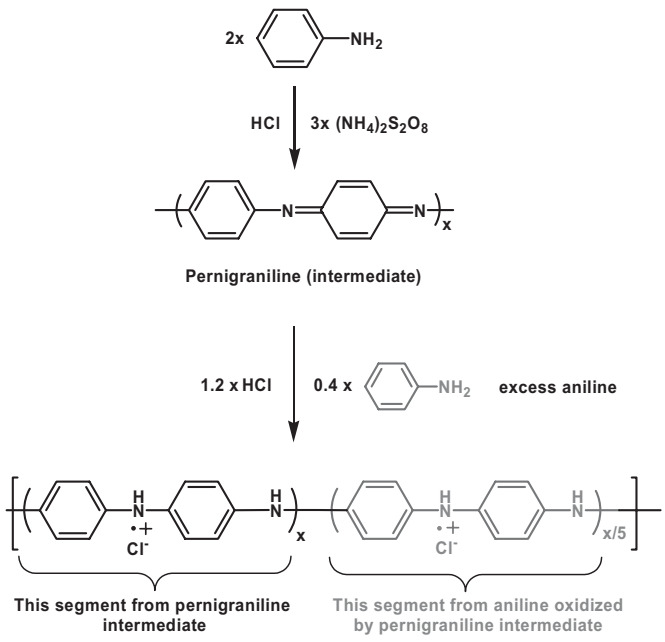

Scheme 2. Two possible routes to emeraldine·HCl segments, one from the reduction of pernigraniline, and the other from oxidative polymerization of aniline by pernigraniline (in gray).

of the $(NH_4)_2S_2O_8$ is also consumed during this process. The remaining 20 % of the polyaniline is obtained as a result of a redox reaction between pernigraniline and fresh aniline that is accompanied by a fall in potential from 0.77 to 0.46 V. There is no additional polymerization beyond this point. Therefore, when $(NH_4)_2S_2O_8$ is added all at once, the bulk of the polyaniline formed (80 %) is a result of oxidation of aniline by $(NH_4)_2S_2O_8$, and the rest, a result of oxidation of aniline by pernigraniline.[12]

In contrast, when $(NH_4)_2S_2O_8$ is added gradually, only the very small amount of polyaniline that is first formed is a result of oxidation of aniline by $(NH_4)_2S_2O_8$. The majority of the polyaniline formed (> 90 %) is a result of oxidation of aniline by pernigraniline. For example, the potential initially rises to 0.76 V consistent with the initial conversion of a small amount of aniline to pernigraniline (nanofibers). The small amount of added $(NH_4)_2S_2O_8$ is completely consumed in this process. The potential then falls from 0.76 to 0.62 V consistent with the redox reaction between pernigraniline and fresh aniline. Subsequent addition of $(NH_4)_2S_2O_8$ arrests any further fall in potential and maintains polyaniline at a sufficiently high oxidation potential to continuously oxidize fresh aniline monomer. From this point on, pernigraniline is the de facto oxidant in the system, and added $(NH_4)_2S_2O_8$ would only play a role in oxidizing emeraldine to pernigraniline, and not to oxidize fresh aniline monomer. The relatively constant polymerization potential of 0.62 V could be viewed as an arbitrary 'hover potential' resulting from an interplay between the effect of added $(NH_4)_2S_2O_8$ that would increase the potential (to 0.76 V), and the redox reaction of pernigraniline with fresh aniline that would decrease the potential (to 0.46 V). After $(NH_4)_2S_2O_8$ addition is complete, the potential of the entire system falls to 0.46 V (emeraldine). Since pernigraniline and not $(NH_4)_2S_2O_8$ is the oxidizing agent in the above system, polyaniline with a granular or nonspecific morphology is obtained.

2.7. *N*-Substituted Polyaniline

The poly(*N*-methylaniline) system provides additional evidence for the aggregation mechanism. Unlike the parent polyaniline system, oxidative polymerization of *N*-methylaniline generally yields a spherical or granular polymer, and even when fibers are obtained, the average fiber diameter is > 300 nm. *N*-Methylaniline is more hydrophobic and more basic than aniline although its oxidation potential is lower than that of aniline. However, the polymerization kinetics of *N*-methylaniline is slower than those of aniline because of steric factors associated with the methyl substituent. These steric barriers should also translate to any *N*-methylaniline/peroxydisulfate aggregates formed in solution which could result in loosely packed aggregates yielding significantly larger average fiber diameters. In addition, because of its higher hydrophobicity, *N*-methylaniline dimer and higher oligomers would precipitate from solution and would promote solid-state polymerization resulting in nonfibrillar polymer growth. This is consistent with fibrillar morphology observed at high dilution and at higher temperatures, where one expects more time for soluble species to aggregate (dilution), or have a greater amount of soluble species that can aggregate (higher temperatures).

Lastly, the mechanistic rationale outlined above can also explain why, under identical experimental conditions, fibrillar polymer growth is not observed in the polypyrrole system. Unlike aniline (pK_a 4.6),[21] pyrrole (pK_a –3.4)[22] is present mainly in its unprotonated form in aqueous 1 M acids and cannot form dimeric aggregates in solution. The large amount of free, unprotonated pyrrole also accounts for the lack of a corresponding induction period, for example, the effective monomer concentration is high resulting in a rapid uncontrolled polymerization that is not conducive to fibrillar polymer growth. In this regard, even in the polyaniline system synthesized at high pH,[23,24] the morphology changes dramatically from nanofibers to nanospheres. At higher pH, there would be a significant amount of free, unprotonated aniline which would result in unregulated polymer growth, and in the absence of repulsive cationic interactions between amine groups, one expects to find significant ortho- and meta-ring coupling along with *N*–*N* azo linkages (as is experimentally observed).[24]

3. Conclusions

This study provides experimental evidence, using LS measurements, that traces the genesis of fibrillar morphology in the polyaniline system to large, colorless aggregates that are formed just prior to the onset of polymerization. A mechanistic model is proposed based on the in situ formation of mono- and dianilinium peroxydisulfate clusters and their subsequent ag-

gregation in solution. While more studies are needed to elucidate their precise chemical constitution, the formation of these aggregates even in the absence of added structure-directing agents such as surfactants, templates, seeds, and so forth, suggests that they could be viewed as in situ generated seeds whose overall shape is transcribed to the bulk precipitate. Unlike previously published studies, we observe a strong temperature dependence in the evolution of fibrillar morphology that can be rationalized by the proposed aggregation-driven mechanism. Confirmatory evidence is obtained from dilution studies. Changes in morphology are amplified in the poly(*N*-methylaniline) system, which underscores the generality of the proposed mechanism. This study also provides insight into why gradual addition of $(NH_4)_2S_2O_8$ does not yield polyaniline nanofibers and why caution should be used in mechanistic interpretations based on the data obtained. This study describes, for the first time, the use of LS measurements for monitoring an oxidative precipitation polymerization system and a new experimental rationale for why the polyaniline system is intrinsically prone to fibrillar polymer growth while other systems, such as polypyrrole, are not.

4. Experimental

Synthesis and Purification: All chemicals were of analytical grade and used as purchased. Bulk synthesis experiments were carried out in 100 mL beakers and LS experiments in 20 mL scintillation vials. A typical room-temperature (RT), salt-free synthesis of polyaniline was carried out as follows. To a magnetically stirred solution of aniline (10.8 mmol) in aqueous 1 M HCl (30 mL) was added, all at once, a solution of ammonium peroxydisulfate (2.60 mM) in aqueous 1 M HCl. The aniline/peroxydisulfate molar ratio was 4:1. After 3 h, the dark-green precipitate of emeraldine·HCl was suction-filtered in air and washed with copious amounts of aqueous 1 M HCl and acetonitrile, followed by air-drying at RT for 30 min and at 80 °C under dynamic vacuum for 12 h. For high-ionic-strength systems, a stock solution of aqueous 1 M HCl containing 3 M NaCl was first prepared and the above procedure was then followed. For experiments requiring continuous monitoring of V_{oc} with time, a Pt foil and a salt bridge (KCl) attached to an SCE reference electrode were immersed in the beaker containing the aniline solution prior to the addition of oxidant, and potential profiling was carried out as described previously. Reactions were carried out at three different temperatures, that is, 0 °C (ice bath), 22 °C (RT), and 55 °C (constant-temperature bath), and three different concentrations for aniline (0.43, 0.22 and 0.022 M) and *N*-methylaniline (0.36, 0.18, and 0.09 M).

LS Measurements: The LS data were obtained by simultaneously monitoring R_g by static LS using the DAWN EOS system and R_h by dynamic LS using the QELS system. Ultrapure water was used to prepare the monomer and oxidant solutions. Both the monomer and oxidant solutions were syringe-filtered (0.2 μm syringe filter, GHP Acrodisc) into a 20 mL glass scintillation vial that was placed in the sample holder of the instrument; the scattering intensity of the polymerizing mixture was continuously monitored with time. For each reaction that was monitored by LS, two identical, simultaneous control reactions were carried out, for example, one equipped for potential profiling (Pt foil, SCE reference, no stirring), and the other for obtaining a visual read on the polymerization (see vials in Fig. 3).

Morphology: The morphology of the polyaniline and poly(*N*-methylaniline) powders was obtained using SEM (Leo 1530VP) and transmission electron microscopy (JEOL 1200EX). For SEM images, a small amount (~1 mg) of the polymer powder was spread in a 1 mm × 1 mm area on a carbon-tab-mounted sample holder and SEM images were obtained without gold coating.

Received: July 23, 2005
Final version: February 7, 2006

[1] X. Zhang, W. J. Goux, S. K. Manohar, *J. Am. Chem. Soc.* **2004**, *126*, 4502.
[2] H. Coelfen, S. Mann, *Angew. Chem. Int. Ed.* **2003**, *42*, 2350.
[3] J. Huang, S. Virji, B. H. Weiller, R. B. Kaner, *J. Am. Chem. Soc.* **2003**, *125*, 314.
[4] X. Zhang, R. Chan-Yu-King, A. Jose, S. K. Manohar, *Synth. Met.* **2004**, *145*, 23.
[5] W. Li, H.-L. Wang, *J. Am. Chem. Soc.* **2004**, *126*, 2278.
[6] X. Zhang, S. K. Manohar, *Chem. Commun.* **2004**, 2360.
[7] a) K. Huang, M. Wan, *Synth. Met.* **2003**, *135–136*, 173. b) S. K. Pillalamarri, F. D. Blum, A. T. Tokuhiro, J. G. Story, M. F. Bertino, *Chem. Mater.* **2005**, *17*, 227.
[8] a) Y. Wang, Z. Liu, B. Han, Z. Sun, Y. Huang, G. Yang, *Langmuir* **2005**, *21*, 833. b) J. Huang, R. B. Kaner, *J. Am. Chem. Soc.* **2004**, *126*, 851.
[9] N.-R. Chiou, A. J. Epstein, *Adv. Mater.* **2005**, *17*, 1679.
[10] J. Huang, R. B. Kaner, *Angew. Chem. Int. Ed.* **2004**, *43*, 5817.
[11] a) Y. Wei, Y. Sun, G. W. Jang, X. Tang, *J. Polym. Sci. Part C* **1990**, *28*, 81. b) L. Duic, M. Kraljic, S. Grigic, *J. Polym. Sci. Part A* **2004**, *42*, 1599.
[12] a) S. K. Manohar, A. G. MacDiarmid, A. J. Epstein, *Synth. Met.* **1991**, *41*, 711. b) L. H. C. Mattoso, O. N. Oliveira, R. M. Faira, S. K. Manohar, A. J. Epstein, A. G. MacDiarmid, *Polym. Int.* **1994**, *35*, 89. c) E. T. Kang, K. G. Neoh, K. L. Tan, *Prog. Polym. Sci.* **1998**, *23*, 277.
[13] D. Chao, J. Chen, X. Lu, L. Chen, W. Zhang, Y. Wei, *Synth. Met.* **2005**, *150*, 47.
[14] J. Appell, G. Porte, *J. Colloid Interface Sci.* **1981**, *81*, 85.
[15] P. J. Wyatt, *Anal. Chim. Acta* **1993**, *272*, 1.
[16] N.-R. Chiou, A. J. Epstein, *Synth. Met.* **2005**, *153*, 69.
[17] X. Zhang, J. Zhang, Z. Liu, C. Robinson, *Chem. Commun.* **2004**, 1852.
[18] R. Atkin, V. S. J. Craig, E. J. Wanless, S. Biggs, *J. Phys. Chem. B* **2003**, *107*, 2978.
[19] S. K. Manohar, X. Zhang, A. Wu, H. Kolla, *Polym. Prepr. (Am. Chem. Soc., Div. Polym. Chem.)* **2004**, *45*, 587.
[20] J. Huang, R. B. Kaner, *Angew. Chem. Int. Ed.* **2004**, *43*, 5817.
[21] F. G. Bordwell, *Acc. Chem. Res.* **1988**, *21*, 456.
[22] Y. Chiang, E. B. Whipple, *J. Am. Chem. Soc.* **1963**, *85*, 2763.
[23] X. Wang, N. Liu, X. Yan, W. Zhang, Y. Wei, *Chem. Lett.* **2005**, 42.
[24] E. J. Behrman, *J. Am. Chem. Soc.* **1967**, *89*, 2424.